PHYS 580 - Computational Physics

Computational Physics by *Nicholas J. Giordano, Hisao Nakanishi*
Student: **Ralph Razzouk**

Lab 8

Problem 1
The starter code `loop.py` provided uses the simple rectangular panel method of integration to compute the magnetic field **B** of a current loop (the Matlab code has two files `loop.m` and `loop_calculate_field.m`). The loop is in the $x - y$ plane and is centered at the origin, just like in the setup discussed in class. (By the way, for this problem, the rectangular panel method is actually the same as the trapezoidal rule. Why?) Extend the programs (or create your own equivalent ones) to calculate the **B** field of two identically shaped parallel loops that share a common axis (the z-axis) and are situated symmetrically about the origin with their respective planes a distance d apart. First, calculate the field when the loops carry equal currents in the same direction, which is the Helmholtz coil configuration that is known to produce a nearly uniform magnetic field at the center. Then, investigate what happens if equal currents are carried in opposite directions.

Solution. The magnetic field of current loops can be calculated using the Biot-Savart law. For a single current loop of radius R in the x-y plane centered at the origin, the magnetic field at any point (x, y, z) is determined by integrating the contributions from infinitesimal current elements around the loop.
For two parallel circular loops with a common axis (the z-axis), we need to calculate the field for each loop separately and then combine them. The loops are positioned symmetrically about the origin at $z = -d/2$ and $z = d/2$.
In the Helmholtz configuration, the currents in both loops flow in the same direction, resulting in a superposition of the magnetic fields

$$\vec{B}_{\text{total}} = \vec{B}_{\text{loop1}} + \vec{B}_{\text{loop2}}.$$

In the anti-Helmholtz configuration, the currents flow in opposite directions

$$\vec{B}_{\text{total}} = \vec{B}_{\text{loop1}} - \vec{B}_{\text{loop2}}.$$

Let's examine the provided code and results for both configurations.
The original code 'loop.py' calculates the magnetic field of a single current loop using numerical integration. The Biot-Savart law is implemented by dividing the loop into small segments and summing their contributions. This approach is equivalent to the trapezoidal rule because each segment is treated as a straight line, with the field contribution calculated at discrete points. The extended code adds the capability to calculate fields for two parallel loops.
Looking at the computational method, for each position (x, y, z), we calculate

$$\vec{B}(x, y, z) = \sum_{i=1}^{N_\phi} \frac{\mathrm{d}\vec{l_i} \times \vec{r}_i}{r_i^3},$$

where $\mathrm{d}\vec{l_i}$ is a small current element and $\vec{r}_i$ is the vector from that element to the point of observation. The sum is taken over N_ϕ angular segments.
In the Helmholtz configuration (Figure 1), we observe that the magnetic field near the origin is remarkably uniform. The B_z component dominates and is nearly constant in the central region between the coils. The plots of B_z along both the z-axis and x-axis confirm this uniformity, showing a flat plateau near the origin. This uniformity is the key characteristic that makes Helmholtz coils valuable in experimental physics, where constant magnetic fields are often required.
For optimal uniformity in Helmholtz coils, the separation distance should be equal to the radius of the loops ($d = R$). This creates a field where the second derivative of B_z with respect to z vanishes at the center, resulting in a particularly flat field profile in the central region.

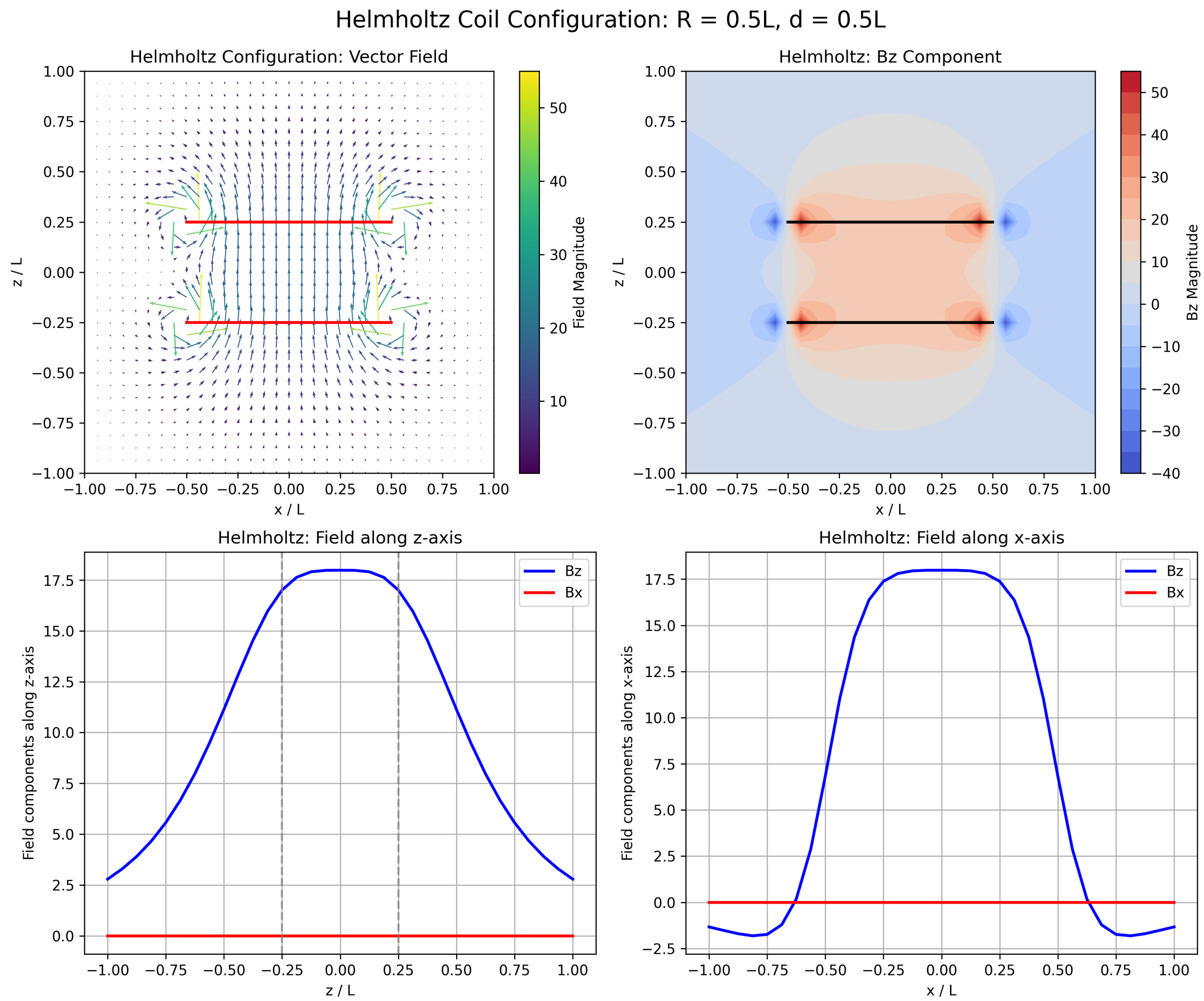

Figure 1: Helmholtz coil configuration with $R = 0.5L$ and $d = 0.5L$. Top left: Vector field plot showing the magnetic field direction and magnitude. Top right: Contour plot of the B_z component. Bottom left: Field components along the z-axis. Bottom right: Field components along the x-axis.

In contrast, the anti-Helmholtz configuration (Figure 2) produces a magnetic field that vanishes at the origin and increases approximately linearly with distance from the center. The B_z component changes sign when crossing the origin along the z-axis, creating a field gradient. The vector field plot clearly shows this behavior, with field lines diverging from the central region. The B_x component exhibits significant magnitude along the x-axis but remains zero along the z-axis due to symmetry.

This linear field gradient characteristic of anti-Helmholtz coils is useful in applications like magnetic traps for neutral atoms (e.g., Magneto-Optical Traps) where force proportional to position is required.

The rectangular panel method used in the code is indeed equivalent to the trapezoidal rule in this case because the integration is performed over the angular parameter ϕ, with equal angular steps $\Delta\phi = 2\pi/N_\phi$. Each segment of the current loop is approximated as a straight line, and the field contribution is calculated at discrete points, which is precisely how the trapezoidal rule works.

In conclusion, the Helmholtz and anti-Helmholtz configurations produce fundamentally different field geometries: Helmholtz coils create a uniform field in the central region, while anti-Helmholtz coils generate a field gradient with zero field at the center. These distinct characteristics make them suitable for different applications in experimental physics and engineering. ∎

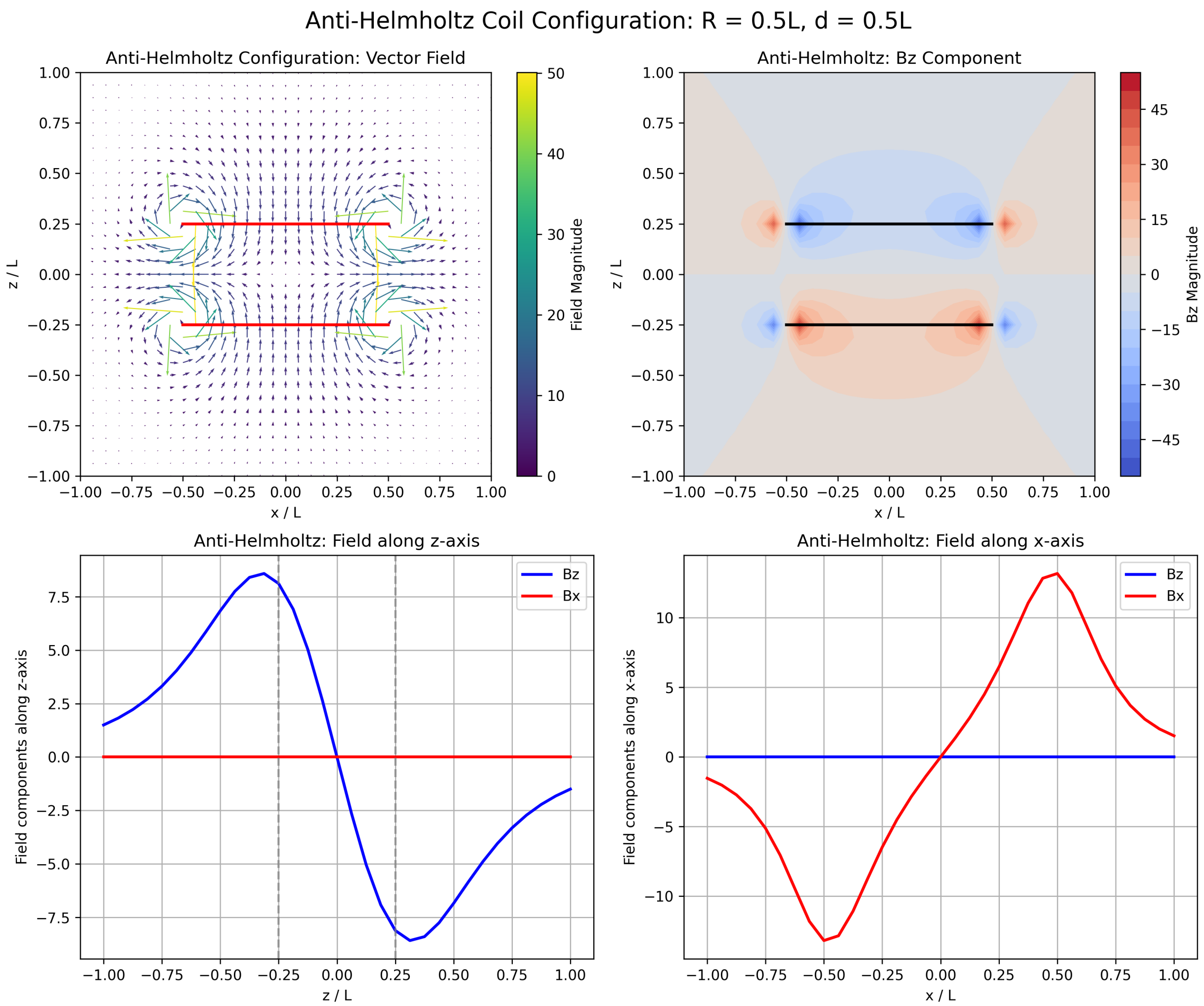

Figure 2: Anti-Helmholtz coil configuration with $R = 0.5L$ and $d = 0.5L$. Top left: Vector field plot showing the magnetic field direction and magnitude. Top right: Contour plot of the B_z component. Bottom left: Field components along the z-axis. Bottom right: Field components along the x-axis.

Problem 2

Extend your programs further to implement the same calculation for a helical coil of multiple loops (i.e., a current-carrying wire wrapped around a cylinder). The coil is centered at the origin, its axis coincides with the z axis, and it has a given pitch P (i.e., the location of the wire advances by distance P in the axial direction as the angle of winding along the wire goes through 2π). Using your program, calculate the magnetic field both inside and outside the coil for various lengths and numbers of winding, with the current set such that $\frac{\mu_0 I}{4\pi} = 1$. Show results for at least one case with loose winding, illustrating how $\boldsymbol{B}$ leaks through the coil, and a case with tight winding, showing how $\boldsymbol{B}$ approaches the field of an ideal solenoid.

Note: The analytic result for $\boldsymbol{B}$ on the axis of an ideal (i.e., tightly wound) solenoid of radius R extending along the z axis from $z = -L/2$ to $L/2$ is

$$B = \hat{e}_z \frac{1}{2}\mu_0 n I \left(\frac{z + L/2}{\sqrt{(z + L/2)^2 + R^2}} - \frac{z - L/2}{\sqrt{(z - L/2)^2 + R^2}} \right),$$

where n is the winding number per unit length and the current I is counter-clockwise when viewed from above the $x - y$ plane. However, away from the axis, for example, at point on the x axis, $\boldsymbol{B}$ is much harder to calculate or approximate analytically (especially when x is of the same order as R).

Solution. To study the magnetic field of a helical coil (solenoid), we implement a numerical calculation based on the Biot-Savart law. The coil is centered at the origin with its axis along the z-axis. It has radius R, length L, and N turns, giving a pitch $P = L/N$. To calculate the magnetic field at any point (x, y, z) due to the helical coil, we discretize the helix into small segments and apply the Biot-Savart law to each segment: $d\vec{B} = \frac{\mu_0}{4\pi}\frac{I d\vec{l} \times \vec{r}}{r^3}$, where I is the current, $d\vec{l}$ is the differential element of the wire, $\vec{r}$ is the position vector from the element to the observation point, and r is its magnitude. For a helical coil, the position of a point on the helix can be parameterized as: $x = R\cos\theta$, $y = R\sin\theta$, $z = -\frac{L}{2} + \frac{P\theta}{2\pi}$, where θ ranges from 0 to $2\pi N$ for N turns.

We present results for two cases: a loosely wound coil with $R = 0.5L_0$, $L = 0.5L_0$, and $N = 1$ turn (pitch $P = 0.5L_0$), and a tightly wound coil with $R = 0.5L_0$, $L = 0.5L_0$, and $N = 500$ turns (pitch $P = 0.001L_0$).

Figure 3 shows the magnetic field for the loosely wound coil. With only one turn, the field pattern resembles that of a current loop more than a solenoid. We observe significant field leakage through the sides of the coil, evident in both the vector field visualization and the B_z contour plot. The field along the z-axis (bottom left) deviates noticeably from the ideal solenoid solution (dashed red line). Additionally, the field along the x-axis (bottom right) shows sharp peaks near the wire location ($x \approx \pm 0.5L_0$). These features are characteristic of a loosely wound coil where the field is dominated by the contribution of individual current elements rather than their collective effect.

Figure 4 shows the magnetic field for the tightly wound coil. With 500 turns, the field pattern closely approaches that of an ideal solenoid. We observe a nearly uniform magnetic field inside the coil, predominantly in the z-direction, with minimal field leakage through the sides. The field lines are mostly contained within the coil volume. The field along the z-axis (bottom left) closely follows the theoretical prediction for an ideal solenoid, while the field along the x-axis (bottom right) shows a characteristic plateau inside the coil with sharp transitions at the coil boundaries ($x \approx \pm 0.5L_0$).

The numerical results for the tightly wound coil match well with the theoretical formula for the field on the axis of an ideal solenoid

$$B_z = \frac{\mu_0 n I}{2} \left(\frac{z + L/2}{\sqrt{(z + L/2)^2 + R^2}} - \frac{z - L/2}{\sqrt{(z - L/2)^2 + R^2}} \right),$$

where $n = N/L$ is the number of turns per unit length. For the tightly wound coil, $n = 500/0.5 = 1000$ turns per unit length, resulting in a strong, uniform magnetic field inside the coil.

The comparison between Figures 3 and 4 clearly demonstrates how the magnetic field structure evolves as the winding density increases. The tight winding produces a much stronger field inside the coil (note the scale difference: maximum $B_z \approx 11$ for loose vs. $B_z \approx 5300$ for tight). The tight winding creates a nearly uniform field inside the coil, while the loose winding has significant spatial variation. Furthermore, the tight

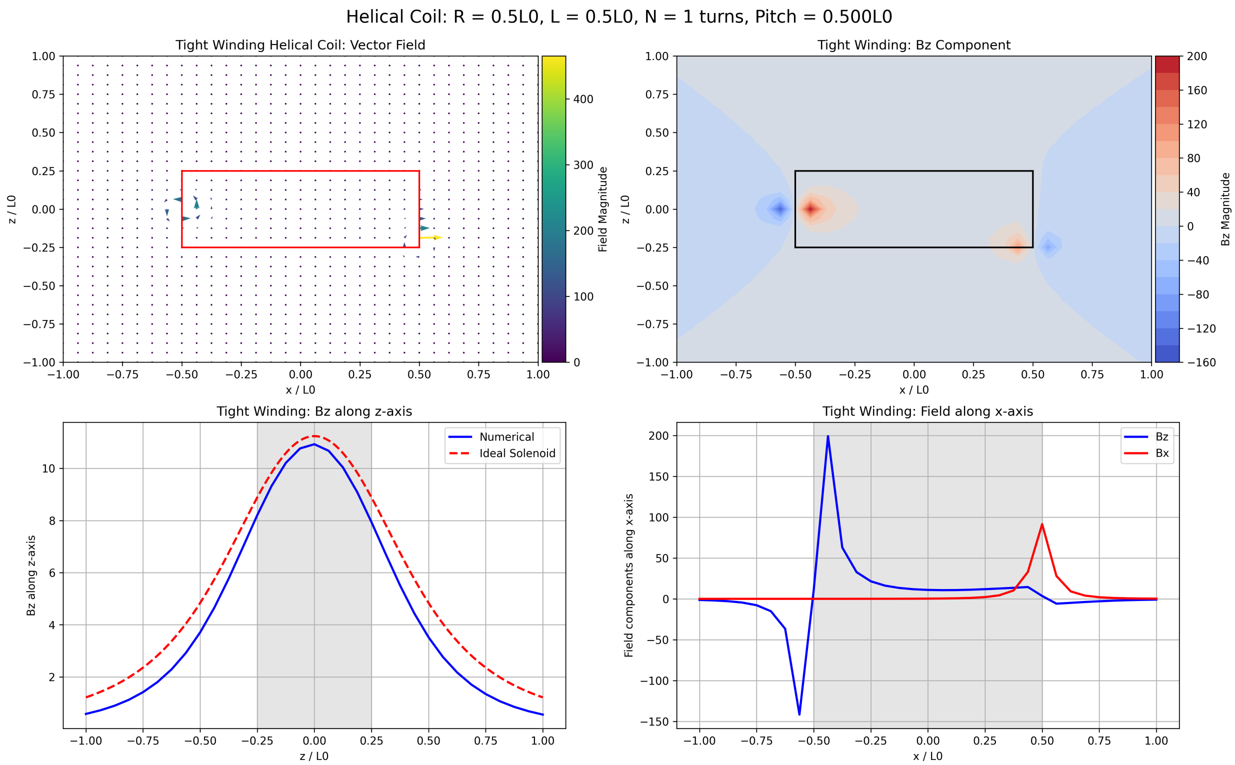

Figure 3: Magnetic field of a loosely wound helical coil with $R = 0.5L_0$, $L = 0.5L_0$, and $N = 1$ turn. Top left: Vector field visualization where arrows indicate field direction and color represents field magnitude. Top right: Contour plot of the B_z component. Bottom left: B_z along the z-axis compared with the ideal solenoid solution. Bottom right: Field components along the x-axis at $z = 0$.

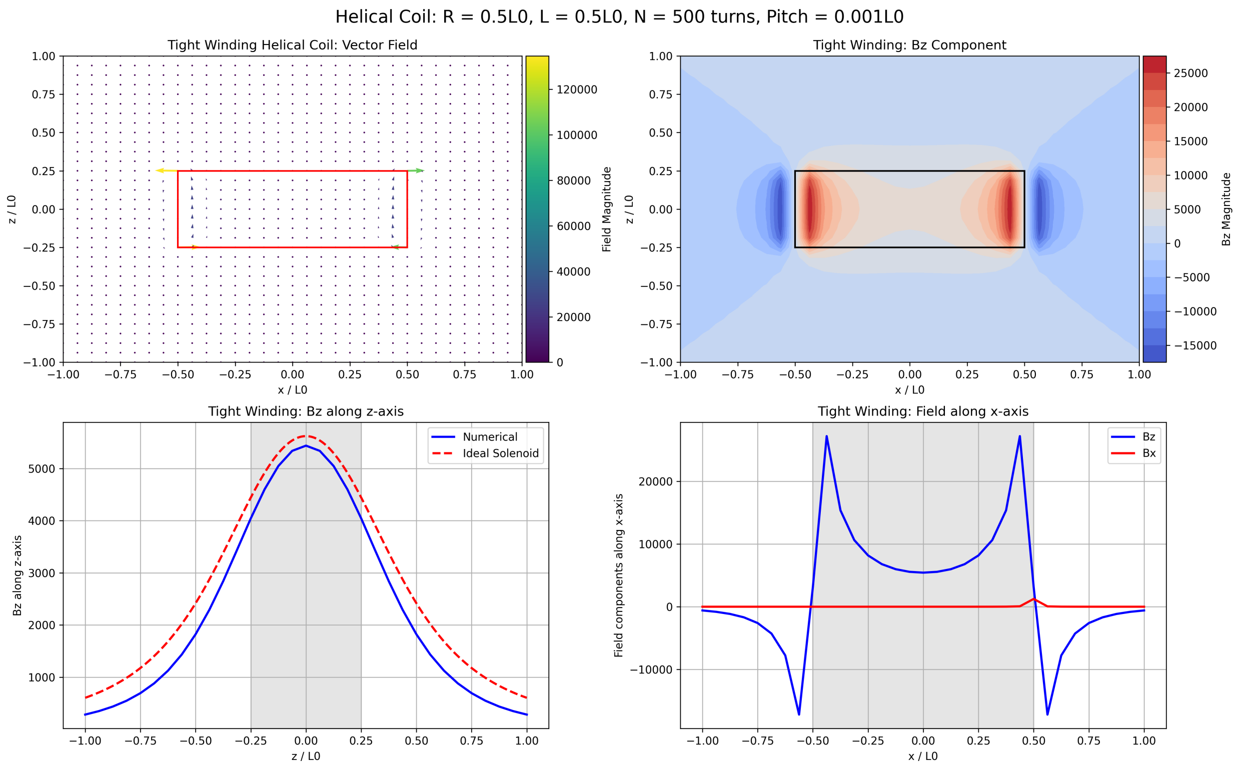

Figure 4: Magnetic field of a tightly wound helical coil with $R = 0.5L_0$, $L = 0.5L_0$, and $N = 500$ turns. Top left: Vector field visualization. Top right: Contour plot of the B_z component showing nearly uniform field inside the coil. Bottom left: B_z along the z-axis closely matching the ideal solenoid solution. Bottom right: Field components along the x-axis at $z = 0$.

winding effectively confines the field within the coil volume, while the loose winding allows substantial field leakage. Both configurations show edge effects at the ends of the coil, but these are proportionally smaller in the tightly wound case.

Our numerical simulations demonstrate the transition from a loosely wound coil, where the magnetic field resembles that of discrete current loops with significant field leakage, to a tightly wound coil that closely approximates an ideal solenoid with a uniform interior field. The simulations confirm the analytical prediction for the on-axis field and provide valuable insights into the full three-dimensional field structure, including regions where analytical solutions are difficult to obtain. The field structure of the tightly wound coil approaches what we expect from an ideal solenoid: uniform magnetic field inside the coil parallel to the axis, and negligible field outside. This behavior is consistent with Ampre's law and the familiar textbook result that $\mathbf{B} = \mu_0 n I \hat{z}$ inside an infinitely long solenoid. Our numerical results also capture the fringing fields near the ends of the finite-length solenoid, which are not accounted for in the simplified infinite-length model. ■